



Short communication

Using a generative adversarial network-based model to simulate fishing behavior in Antarctic krill fishery

Fanyi Meng^{a,b}, Guoping Zhu^{a,b,c,d,*}^a College of Marine Living Resource Sciences and Management, Shanghai Ocean University, Shanghai 201306, China^b Center for Polar Research, Shanghai Ocean University, Shanghai 201306, China^c National Engineering Research Center for Oceanic Fisheries, Shanghai 201306, China^d Polar Marine Ecosystem Group, The Key Laboratory of Sustainable Exploitation of Oceanic Fisheries Resources, Shanghai Ocean University, Ministry of Education, Shanghai 201306, China

ARTICLE INFO

Handled by Jie Cao

Keywords:

Fishing behavior
Generative adversarial network
Krill fishery
Fishing ground

ABSTRACT

The existing implementation of a management policy for Antarctic krill fishery has faced challenges due to the diverse and variable management strategies. Understanding the fishing behavior of krill fishery is crucial for developing sustainable policies. In this study, krill fishery data collected on the Antarctic Peninsula, where is the key fishing ground, was used to model krill fishing behavior using generative adversarial networks (GANs). The GANs successfully captured fishing behavior, particularly important features such as temporal characteristics and the Lévy flight, and the performance was better than the previous approaches. Overall, this modeling approach shows promise as a tool for monitoring fishing behavior and management of krill fishery in the Southern Ocean.

1. Introduction

Antarctic krill (*Euphausia superba*) is a keystone species in the Southern Ocean ecosystem and plays a crucial role in the region's fishing industry due to its large biomass and wide distribution (Santa Cruz et al., 2018; Wang and Zhu, 2019). The Commission for the Conservation of Antarctic Marine Living Resources (CCAMLR) has been responsible for managing the krill fishery since the early 1980s. Initially, catch limits according to subareas were set to effectively prevent the depletion of krill resources. However, with the increasing influx of fishing effort into the Southern Ocean, maintaining a balance between the fisheries economy and the Southern Ocean ecosystem has become increasingly important (Kawaguchi and Candy, 2009; Wang and Zhu, 2019). Thus, decoding the intricacies of krill fishing behavior becomes an imperative endeavor, providing crucial insights to assist CCAMLR in effectively stewarding the krill fishery.

Behavior modeling is particularly important in ecology as it helps explain the underlying mechanisms behind behavior and clarifies ecological processes at the population level (Nathan et al., 2008). In the past, fishing behavior was studied through purely statistical approaches that focused on the static distribution of fishing behavior, such as assessing local vessel activity based on costs and profits in the Gulf of Mexico (Weninger and Perruso, 2013). In other regions, fishery resource

distribution is considered as a more common statistical parameter (Marín and Delgado, 2001; Tabeta et al., 2015). A more advanced approach involves simulating fishing behavior by considering the interaction between vessels and their environment. An example in the krill fishery include modeling fishing behavior was based on assumptions related to sea ice extent (Santa Cruz et al., 2018). While these studies have achieved good results, such traditional statistical models may face challenges in parameter estimation, especially as the complexity of the model increases (e.g., considering numerous environmental factors). Additionally, specific assumptions simplify fishing behavior inevitably, leading to the omission of key characteristics of real-world scenarios. For instance, previous models primarily focused on spatial modeling of fishing behavior, largely ignoring the temporal variation in fishing behavior, which is equally important. Moreover, recent study underscores a reality: despite substantial advancements in technology, such as sonar, echo sounders, and satellite communications, the uncertainty of fish locations remains a persistent challenge. This uncertainty compels fishing vessels to adopt a search strategy reminiscent of other predators, characterized by Lévy flights (Bertrand et al., 2007; Kawaguchi et al., 2009; Kawaguchi and Nicol, 2020). However, this inherent characteristic of fishing behavior has not been adequately accounted for in modeling fishing behavior. To address these issues, data-driven methods such as deep learning (DL) have gained increasing

* Corresponding author at: College of Marine Living Resource Sciences and Management, Shanghai Ocean University, Shanghai 201306, China.

E-mail addresses: 1929424@st.shou.edu.cn (F. Meng), gpzhu@shou.edu.cn (G. Zhu).

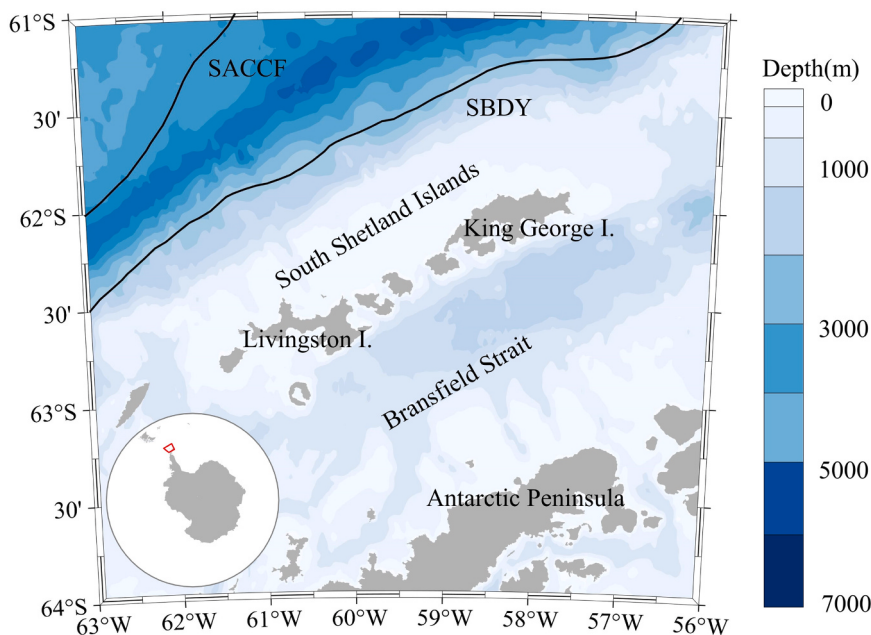


Fig. 1. Map of study area, which is identified by the red box in the Southern Ocean. Climatological position of the Southern Antarctic Circumpolar Current Front (SACCF) and Southern Boundary front (SBDY) are indicated in black according to Kim and Orsi (2014).

Table 1
Fishing information of Chinese krill trawlers in the FAO Statistical Subarea 48.1 during 2019–2021.

Year	Date of starting fishing	Date of ending fishing	Number of nets
2019	28 March	10 June	626
2020	9 March	30 June	883
2021	15 March	4 June	769

attention.

DL is a multilayer neural network architecture that transcends the limitations of covariates, which learn global features from a large amount of data without predefined complex rules (Cao et al., 2019; Gao et al., 2022b). One of DL models, generative adversarial networks (GANs), has been widely used not only in fields such as image generation and target detection (Hu et al., 2018; Kim and Myung, 2018; Zhan et al., 2018), but also in simulating motion trajectories (Gao et al., 2022b). GANs are cutting-edge approaches that generates a plethora of data and

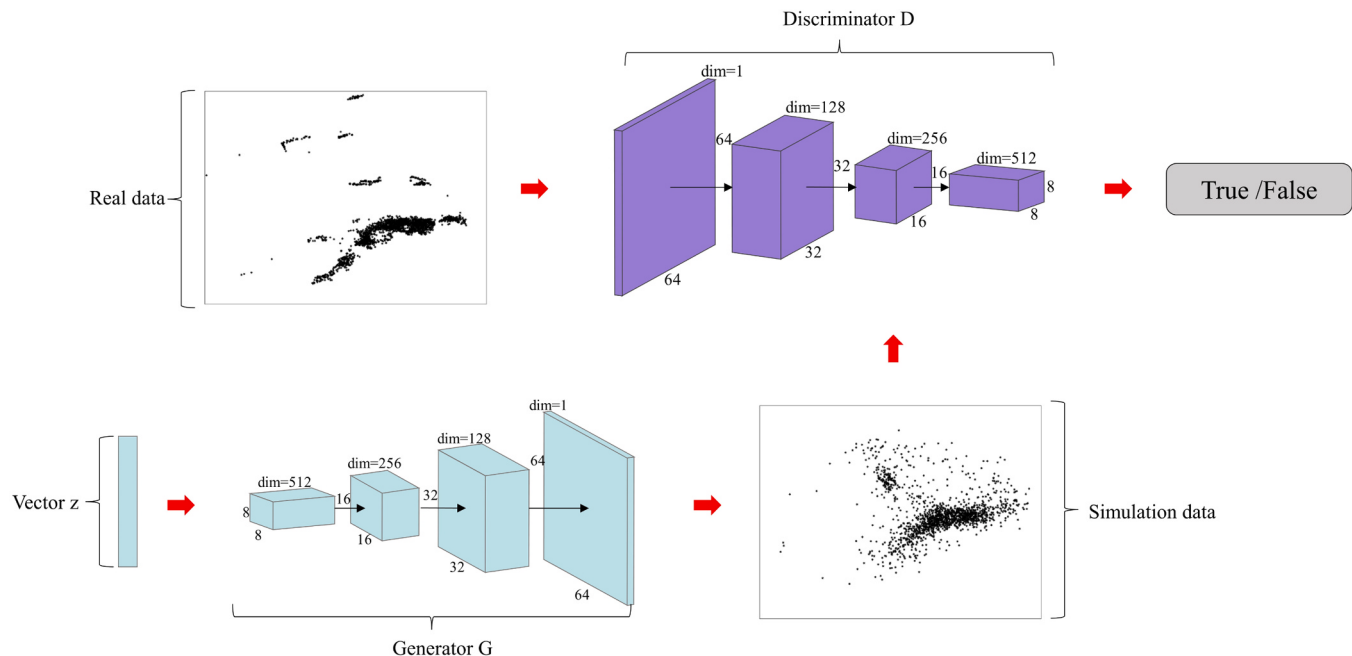


Fig. 2. Visualized summary of GAN framework. In each iterative cycle, a random vector z (represented in yellow) is fed into the generator G. Through several convolution operations (indicated in blue), this vector is transformed into the dimensionality of the simulated data. Both the simulated data and the real data are then randomly input into the discriminator D. The discriminator D processes these inputs, elevating their dimensionality to discern whether the data is real or generated. This information is subsequently utilized to optimize the training in the next iteration, enhancing the model's ability to simulate complex patterns such as fishing behavior.

have been applied to simulate the motion trajectories of urban residents (Atluri et al., 2018; Duan et al., 2014). Recently, GANs have also been used to simulate central-place foraging trajectories of seabirds, outperforming traditional statistical models (Roy et al., 2022). Inspired by these observations, this study aims to use GANs to model fishing behavior in krill fishery to help address existing methodological issues and effectively capture key features.

2. Materials and methods

2.1. Data sources

The Chinese krill fishery data from the northern Antarctic Peninsula, specifically the FAO Statistical Subarea 48.1, was collected for the years 2019–2021 (Fig. 1). During this period, vessels conduct 759.33 ± 128.77 (mean \pm standard deviation) tows in the cold seasons, specifically from March to June (Table 1).

The raw data comprises the essential data fields to develop the model, including the date of fishing operation, as well as latitude and longitude of start and end fishing. The data underwent a preprocessing step using Roy et al.'s (2022) GAN format. During this preprocessing step, the data was linearly re-interpolated with a fixed time step length of 2 h. It was then divided into 14 equally sized groups and the operating points were determined as the midpoint of trawl positions. These operating points were normalized and used as the latitude and longitude coordinates. Each group of data was then padded to create a 200×200 matrix, with a default value of 0. This matrix representation allows for further analysis and modeling of the fishing behavior. Overall, this preprocessing step ensures that the data is in a suitable format for analysis and modeling using GANs as described in the subsequent sections of this study.

Additionally, daily Sea Ice Concentration (SIC) data with spatial resolution of 25 km, sourced from the National Snow and Ice Data Center (NSIDC; Meier et al., 2021), were used to evaluate seasonal dynamics of sea ice in the Statistical Subarea 48.1.

2.2. Model building

GANs are a type of neural network architecture used for generating synthetic data, as illustrated in Fig. 2. They consist of two main components: a generator (G) and a discriminator (D). The generator takes a noise vector as input and generates simulation data, while the discriminator distinguishes between real and simulated data (Radford et al., 2016). The process can also be mathematically represented as follows,

$$\min_G \max_D V(D, G) = E_{x \sim P_{\text{data}}(x)} [\log D(x)] + E_{z \sim P_z(x)} [\log(1 - D(G(z)))] \quad (1)$$

where $P_{\text{data}(x)}$ and $P_z(x)$ are the probability distributions of the real and simulation data, respectively. During the training process, GANs create a game-like scenario where the generator tries to generate data that can fool the discriminator, while the discriminator aims to correctly classify the real and simulation data. This adversarial competition between the generator and discriminator helps the network to learn and generate increasingly realistic data.

The baseline GAN (hereinafter as “baseline model”) has challenges in capturing the spectrum of real data, leading to potential degradation in output quality (Durall et al., 2020). To overcome this issue and enhance model stability, we developed a spectral-regularized GAN (hereafter referred to as the “regularization model”), inspired by the approach proposed by Durall et al. (2020). The regularization model introduces a spectral loss $\mathcal{L}_{\text{spectral}}$ to constrain the generator G and enhance the learning of the data spectrum,

$$\mathcal{L}_{\text{spectral}} = \sum [\log(F(x_0, \dots, x_n)) - \log(F(\hat{x}_0, \dots, \hat{x}_n))]^2 \quad (2)$$

where F is the Fourier transform function of the two-dimensional matrix,

x and \hat{x} are real and simulation data, respectively.

2.3. Evaluation metric

To evaluate the stability of GANs training, we employed a method to track the loss values of the generator and discriminator at each iteration. Specifically, these loss values were computed based on a randomly selected subset of the training data,

$$\mathcal{L} = \frac{1}{m} \sum_m [\log(D(x)) + \log(1 - D(G(z)))] \quad (3)$$

where \mathcal{L} is the loss function, m is the subset, and x and z are the real data and noise vector, respectively. A bootstrap sampling approach was introduced to further ensure robust evaluation. The mean and standard deviation of the loss values over all bootstrap samples were reported. The loss values also serve as an indicator of the fitness of GANs, where values below 1 are regarded as indicative of a good fit, and lower values are preferred. To ensure a robust evaluation, we introduced a bootstrap sampling approach. This involved resampling the dataset 100 times to create bootstrap samples, from which the loss values were calculated. The mean and standard deviation of the loss values were then reported, providing a comprehensive assessment of the GANs model's performance.

In addition, we employed three methods to assess the quality of the simulation data. These methods were implemented as follows:

- a) Inspection of the Fourier distribution by Fourier transforming in longitude and latitude, with the spectrum estimated based on the periodogram method,

$$X(\omega) = \sum_{n=0}^{N-1} X(n) e^{-j\omega n} \quad (4)$$

$$\log_{10} \widehat{S}(\omega) = \log_{10} \frac{1}{N} |X(\omega)|^2 \quad (5)$$

where $\widehat{S}(\omega)$ is the spectral estimate, N is the total sample size, and $X(n)$ and $X(\omega)$ are the datasets before and after the Fourier transform, respectively.

- b) Verification of the Lévy flight, which relies on characterizing the statistical distribution of step lengths between successive operating points by means of an inverse power law distribution:

$$P(l) \sim l^{-\mu} \quad (6)$$

where $P(l)$ is the probability of move length l and the μ value indicates the type of motion, i.e., $\mu \geq 3$ corresponds to the Brownian motion, $\mu \leq 1$ is close to a ballistic motion, and $1 < \mu < 3$ corresponds to Lévy flights.

Building the histogram of the step length frequency is a popular method to estimate the value of μ , which is also the reversed slope of the log-log plot of the long-tailed distribution (discarding the first two bins of the histogram). Routinely, histograms were constructed using Scott's rule (Scott, 1979) to minimize the mean squared error of density estimation,

$$h = 3.5 \cdot SD \cdot N^{-1/3} \quad (7)$$

where N is the total sample size, SD is the standard deviation of the sample, and h is the histogram's bin width.

- c) Characterization of the spatiotemporal distribution. The approach of Kawaguchi and Candy (2009) was used to determine the fishing ground. Specifically, a fishing ground is characterized by the presence of a core area with operating points less than 2 km apart and more than 200 operating points within a radius of 55 km.

All data were performed in Python (version 3.9).

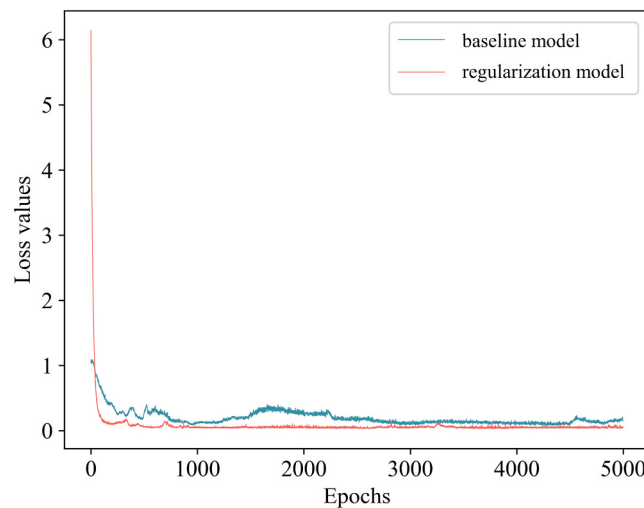


Fig. 3. Loss values convergence of baseline and regularization models over 5,000 epochs.

3. Results

Throughout the extensive training period of 5000 epochs, both the baseline model and the regularization model consistently maintained stability, resulting in loss values that effectively converged to 0 (Fig. 3). Importantly, the baseline model recorded an average loss value of 0.1282 ($SD = 0.0278$), whereas the regularization model showcased superior performance with an average loss value of 0.0488 ($SD = 0.0081$), affirming their successful fitting capabilities.

To evaluate the quality of the simulated data, we examined the Fourier distribution, statistical distribution, and conducted visual inspections. The Fourier distribution of the real and simulation data generally aligned. In the low-frequency band, the baseline and regularization models demonstrated similar fitting abilities. However, in the high-frequency band, the regularization model outperformed, particularly evident in the latitudinal spectrogram (Fig. 4).

The analysis of statistical distribution reveal that the simulation data from both the baseline and regularization models demonstrated a characteristic long-tailed distribution akin to real fishing data, indicating their ability to capture the spatio-temporal patterns of fishing behavior. Moreover, both real and simulation fishing behaviors adhered to Lévy flights, as indicated by the μ values (1.469, 2.855, and 2.441) falling within the range of 1–3 (Fig. 5).

Visual inspection of the fishing behavior from 2019 to 2021 reveals a concentration of fishing activities primarily around the South Shetland Islands, with a noticeable trend towards the north shelf area of the Antarctic Peninsula, which corresponds to the location of the fishing grounds. This variation pattern of fishing behavior is also captured in the simulation data (Fig. 6).

4. Discussion

The GANs have emerged as a revolutionary force in the realm of DL, showcasing remarkable versatility across an array of domains, from image generation to target detection, and even in the intricate art of spatio-temporal modeling (Cao et al., 2019; Gao et al., 2022b). The prowess of GANs extends to the resolution of complex ecological conundrums, excelling in the simulation of non-linear data, such as the generation of biotic imagery and seabird movement trajectories (Lu et al., 2019; Madsen et al., 2019; Roy et al., 2022). These advancements underscore the promise of GANs as a potent instrument for simulating fishing behavior.

The intricate nature of fisheries exploitation, coupled with its profound impact on marine ecosystems, makes modeling fishery behavior an imperative yet formidable undertaking (Trathan et al., 2021; Wang and Zhu, 2019). With regard to the krill fishery, its spatio-temporal patterns — influenced by diverse factors such as krill distribution, sea ice pattern, and catch levels — prove challenging to predict. Chinese krill fishing vessels operating in Subarea 48.1 during the cold seasons from 2019 to 2021 demonstrated significant alterations in spatial patterns, despite consistent sea ice dynamics (Figure S1). Moreover, the 2018–19 synoptic survey (Kraft et al., 2021) highlighted a high concentration of krill in the vicinity of the South Shetland Islands, suggesting that krill distribution was not the primary impetus for vessels'

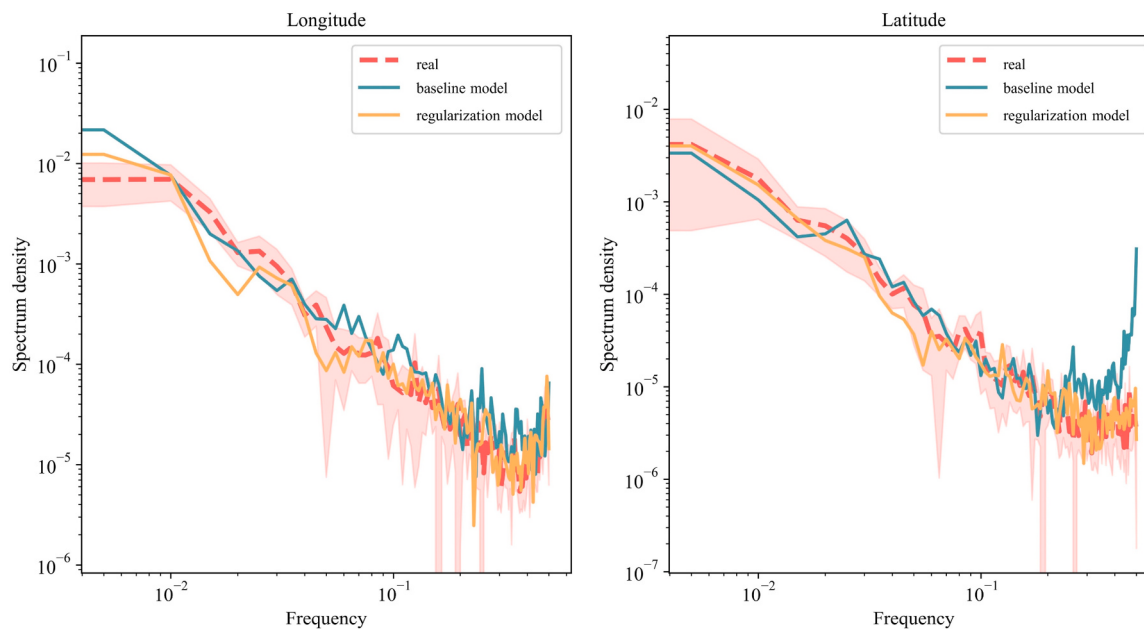
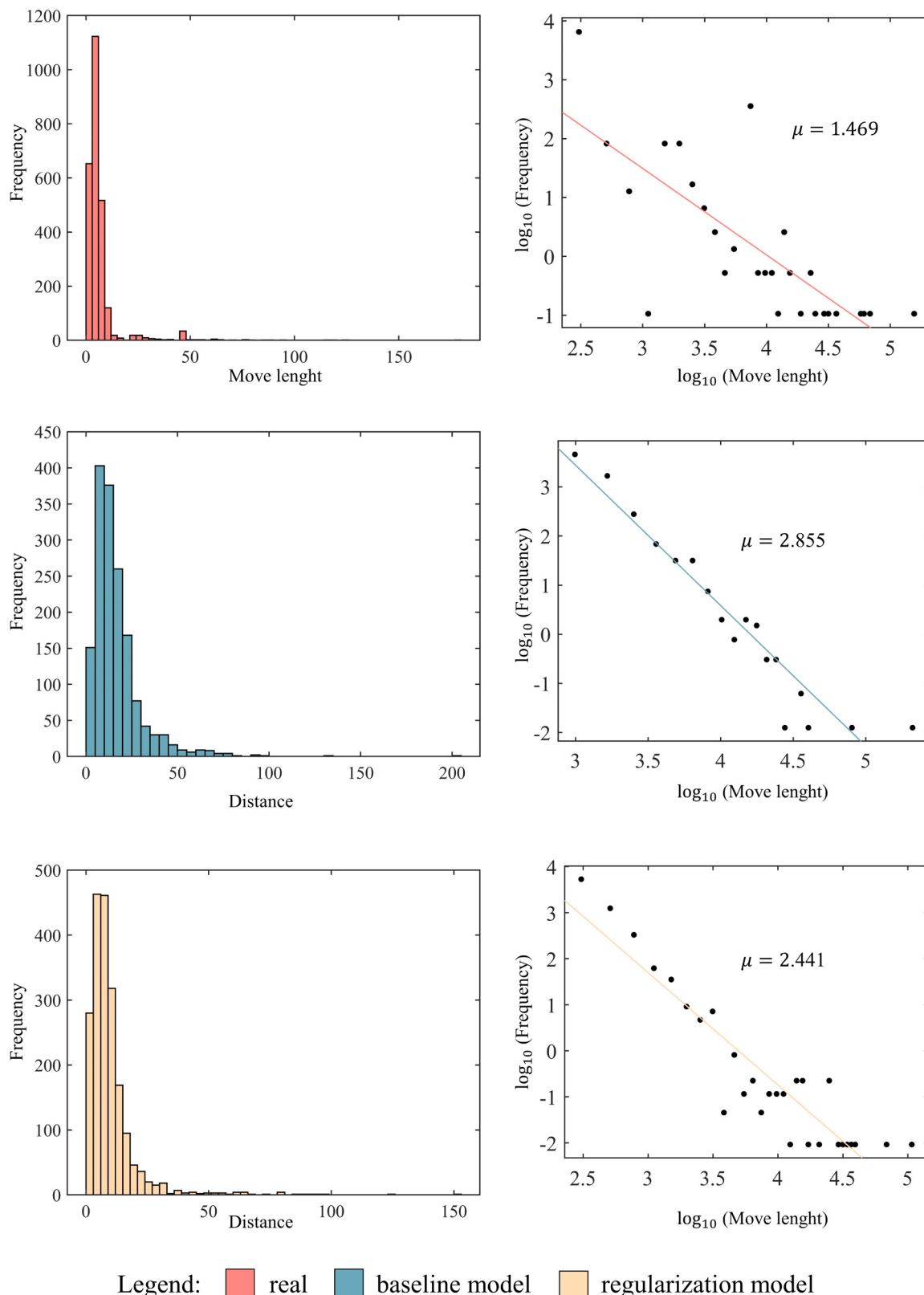


Fig. 4. The data is presented in the form of a Fourier distribution, with separate distributions for the longitude and latitude directions (as indicated by the headings above the panel). The red dashed line represents the real data, while the blue solid line and yellow solid line represent data generated by the baseline model and regularization model, respectively. The red shaded area illustrates the standard deviation of the real data.



Legend: real baseline model regularization model

Fig. 5. The histogram on the left displays the statistical distribution of move-lengths, while the corresponding values of u are shown on the right. The red, blue, and yellow colors correspond to real data, baseline model-generated data, and regularization model-generated data (as indicated in the legend).

southern movement. Although the inclusion of more factors into the model might enhance the representation of fishery behavior, the resultant increased complexity may amplify the deviation from the actual scenario (Fielding et al., 2014).

GANs propose an alternative methodology to capture pivotal features by learning the latent processes underlying behavior (Gao et al., 2022b; Roy et al., 2022). Our results, corroborated by the previous study (Wang and Zhu, 2019), suggest a marked preference among Chinese krill

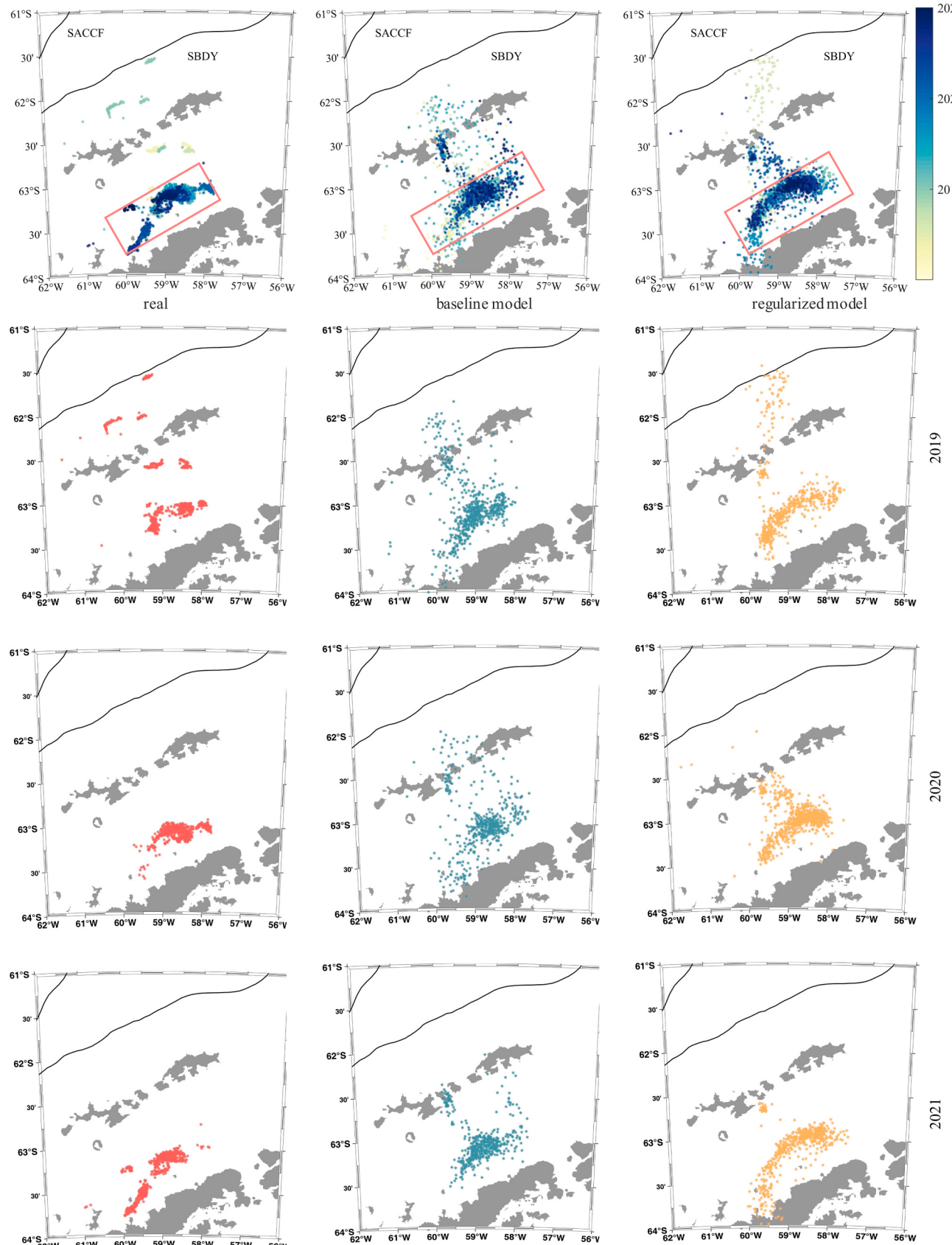


Fig. 6. Spatial-temporal distribution is shown from left to right, with real data, baseline model-generated data, and regularization model-generated data, respectively; and is shown from up to down, with all years' distribution, annual year's distribution respectively. Operating points that occur at different times are highlighted in different colors (as shown on the color bar). The red box outlines the extent of the fishing grounds. Climatological position of the Southern Antarctic Circumpolar Current Front (SACC) and Southern Boundary front (SBDY) are indicated in black according to Kim and Orsi (2014).

fishing vessels to fish in the vicinity of the South Shetland Islands and in the Bransfield Strait, all those adhering to Lévy flights. The efficacy of GANs in capturing the Lévy flights and spatio-temporal pattern of fishing behavior in krill fishery is evident in our study, and spectral regularization further enhances its performance, which is a feat that traditional statistical models find challenging to match. Meanwhile, the extra metrics, Fourier distribution and detection of fishing grounds, also demonstrate that models' result align with the real data. It's noted that the variability and randomness in evaluation results include Fourier distribution's frequency, μ values, and the range of fishing grounds, should be viewed as beneficial. These variations within acceptable bounds underscore that GANs has internalized the distribution of the real data, rather than merely replicating it (Arjovsky et al., 2017).

Our attention is drawn to the fact that, despite the robust capabilities of our method in capturing the macroscopic features of fishing behavior, it has difficulties simulating fine-scale features as previous models do. The GANs' recognition of topography leaves room for improvement, though spectral regularization does enhance its performance significantly (Fig. 6). It falls short of avoiding land exclusively, as geography-based models such as the geographic weighting model are known to do.

We envisage two potential solutions to these challenges. First, refining the internal structure of GANs by gleaning insights from other derived models, such as the comparison of the similarity between real and simulated distribution probabilities in terms of Earth mover's distance (Wasserstein GAN) (Arjovsky et al., 2017), or the computation of loss values using least squares loss functions (Least Squares GAN) (Mao et al., 2017). Second, integrating other models, such as spatial statistical models known for their superior location information processing capabilities, into GANs could potentially address the GANs' deficiency in spatial cognition at fine-scale levels.

While our proposed model may not be without its flaws, we anticipate it to make inroads in addressing critical ecological challenges in the future, especially those related to the Southern Ocean fisheries. Fishery distribution estimation forms a crucial component of ecosystem risk assessment frameworks. For krill fishery, the GANs is superior to the regular practice of using historical catch data averages to represent current fishery distribution (Marín and Delgado, 2001; Warwick-Evans et al., 2022a). Therefore, this offers a flexible fishery distribution for risk assessment frameworks, facilitating the testing of the resilience of fishery management policies. Furthermore, in studies delving into the mechanisms behind fishery behavior (Hofmann and Murphy, 2004; Warwick-Evans et al., 2022b), the GANs discriminator could potentially take on a role analogous to the calibration of observational data, courtesy of its prowess in evaluating result authenticity.

5. Conclusions

The GANs is a straightforward yet impressive model that accurately simulates fishing behavior, outperforming existing approaches in capturing the distinctive traits of fisheries. It also stands as an exceptionally flexible tool, providing substantial benefits to the improvement and diversification of current studies, such as the exploration of underlying mechanisms of fishing behavior and risk assessment of fishery management strategies. Nevertheless, there are still areas where the model could be refined, particularly concerning the learning of fine-scale features. Employing approaches like spectral regularization, which modify the neural network's structure, may potentially resolve this challenge.

Compliance with ethical standards

None.

Human and animal rights

All applicable international, national, and/or institutional guidelines

for the care and use of animals were followed.

CRediT authorship contribution statement

Fanyi Meng: Writing – review & editing, Writing – original draft, Visualization, Validation, Software, Methodology, Formal analysis, Conceptualization. **Guoping ZHU:** Writing – review & editing, Writing – original draft, Validation, Supervision, Resources, Project administration, Methodology, Funding acquisition, Data curation, Conceptualization.

Declaration of Competing Interest

The authors declare that they have no conflict of interest.

Data Availability

Data will be made available on request.

Acknowledgements

We also are grateful to the captains of large-scale krill trawlers and the scientific observers onboard those vessels for sampling and collecting data. Team members of the Polar Marine Ecosystem Laboratory, Shanghai Ocean University deserves special recognition for their efforts in the laboratory. We further thank the College of Marine Living Resource Sciences and Management at Shanghai Ocean University for providing the facilities in the laboratory that make this study happen. This project was supported by the 'Inter-governmental Science and Technology Innovation (STI) Cooperation Special Programme' of the National Key Research and Development Programme (grant no 2023YFE0104500 to G.P. Zhu) and the National Natural Science Foundation of China (grant 41776185 to G.P. Zhu).

Appendix A. Supporting information

Supplementary data associated with this article can be found in the online version at doi:10.1016/j.fishres.2024.107065.

References

- Arjovsky, M., Chintala, S., Bottou, L., 2017. Wasserstein GAN. ArXiv E-Prints arXiv: 1701.07875. <https://doi.org/10.48550/arXiv.1701.07875>.
- Atluri, G., Karpatne, A., Kumar, V., 2018. Spatio-temporal data mining: a survey of problems and methods, 83:1-83:41 ACM Comput. Surv. 51. <https://doi.org/10.1145/3161602>.
- Bertrand, S., Bertrand, A., Guevara-Carrasco, R., Gerlotto, F., 2007. Scale-invariant movements of fishermen: the same foraging strategy as natural predators. Ecol. Appl. 17, 331–337. <https://doi.org/10.1890/06-0303>.
- Cao, Y.-J., Jia, L.-L., Chen, Y.-X., Lin, N., Yang, C., Zhang, B., Liu, Z., Li, X.-X., Dai, H.-H., 2019. Recent advances of generative adversarial networks in computer vision. IEEE Access 7, 14985–15006. <https://doi.org/10.1109/ACCESS.2018.2886814>.
- Duan, Y., Lv, Y., Kang, W., Zhao, Y., 2014. A deep learning based approach for traffic data imputation, in: 17th International IEEE Conference on Intelligent Transportation Systems (ITSC). Presented at the 17th International IEEE Conference on Intelligent Transportation Systems (ITSC), pp. 912–917. <https://doi.org/10.1109/ITSC.2014.6957805>.
- Durall, R., Keuper, M., Keuper, J., 2020. Watch Your Up-Convolution: CNN Based Generative Deep Neural Networks Are Failing to Reproduce Spectral Distributions. Presented at the Proceedings of the IEEE/CVF Conference on Computer Vision and Pattern Recognition, pp. 7890–7899.
- Fielding, S., Watkins, J.L., Trathan, P.N., Enderlein, P., Waluda, C.M., Stowasser, G., Tarling, G.A., Murphy, E.J., 2014. Interannual variability in Antarctic krill (*Euphausia superba*) density at South Georgia, Southern Ocean: 1997–2013. ICES J. Mar. 71, 2578–2588. <https://doi.org/10.1093/icesjms/fsu104>.
- Gao, N., Xue, H., Shao, W., Zhao, S., Qin, K.K., Prabowo, A., Rahaman, M.S., Salim, F.D., 2022b. Generative adversarial networks for spatio-temporal data: a survey, 22:1-22: 25 ACM Trans. Intell. Syst. Technol. 13. <https://doi.org/10.1145/3474838>.
- Hofmann, E.E., Murphy, E.J., 2004. Advection, krill, and Antarctic marine ecosystems. Antarct. Sci. 16, 487–499. <https://doi.org/10.1017/S0954102004002275>.
- Hu, D., Wang, L., Jiang, W., Zheng, S., Li, B., 2018. A Novel Image Steganography Method via Deep Convolutional Generative Adversarial Networks. IEEE Access 6, 38303–38314. <https://doi.org/10.1109/ACCESS.2018.2852771>.

- Kawaguchi S., Candy S., Constable C. (2009) Characterising krill fishery dynamics using a random walk model. WG-EMM-09/18. Commission for the Conservation of Antarctic Marine Living Resources, Hobart, Tasmania, Australia.
- Kawaguchi, S., Candy, S., 2009. Quantifying movement behaviour of vessels in the Antarctic krill fishery. CCAMLR Sci. 16, 131–148.
- Kawaguchi, S., Nicol, S., 2020. Krill Fishery. In: Lovrich, G., Thiel, M., (Eds), Fisheries and Aquaculture. Oxford University Press, Oxford. 137–158. doi: 10.1093/oso/9780190865627.003.0006.
- Kim, K., Myung, H., 2018. Autoencoder-Combined Generative Adversarial Networks for Synthetic Image Data Generation and Detection of Jellyfish Swarm. IEEE Access 6, 54207–54214. <https://doi.org/10.1109/ACCESS.2018.2872025>.
- Kim, Y.S., Orsi, A.H., 2014. On the variability of Antarctic circumpolar current fronts inferred from 1992–2011 altimetry. J. Phys. Oceanogr. 44, 3054–3071.
- Krafft, B.A., Macaulay, G.J., Skaret, G., Knutson, T., Bergstad, O.A., Lowther, A., Huse, G., Fielding, S., Trathan, P., Murphy, E., Choi, S.-G., Chung, S., Han, I., Lee, K., Zhao, X., Wang, X., Ying, Y., Yu, X., Demianenko, K., Podhorny, V., Vishnyakova, K., Pshenichnov, L., Chuklin, A., Shyshman, H., Cox, M.J., Reid, K., Watters, G.M., Reiss, C.S., Hinke, J.T., Arata, J., Godø, O.R., Hoem, N., 2021. Standing stock of Antarctic krill (*Euphausia superba* Dana, 1850) (*Euphausiacea*) in the Southwest Atlantic sector of the Southern Ocean, 2018–19. J. Crustac. Biol. 41, 1–17. <https://doi.org/10.1093/jcbiol/rua046>.
- Lu, C.-Y., Rustia, D.J.A., Lin, T.-T., 2019. Generative adversarial network based image augmentation for insect pest classification enhancement. IFAC-Pap. 52, 1–5.
- Madsen, S.L., Dyrmann, M., Jørgensen, R.N., Karstoft, H., 2019. Generating artificial images of plant seedlings using generative adversarial networks. Biosyst. Eng. 187, 147–159.
- Mao, X., Li, Q., Xie, H., Lau, R.Y., Wang, Z., Paul Smolley, S., 2017. Least squares generative adversarial networks. Presented Proc. IEEE Int. Conf. Comput. Vision 2794–2802.
- Marín, V.H., Delgado, L.E., 2001. A spatially explicit model of the Antarctic krill fishery off the South Shetland Islands. Ecol. Appl. 11, 1235–1248. <https://doi.org/10.2307/3061024>.
- Meier, W.N., Fetterer, F., Windnagel, A.K., Stewart, J.S., 2021. NOAA/NSIDC Climate Data Record of Passive Microwave Sea Ice Concentration, Version 4 [Data Set]. Boulder, Colorado USA. National Snow and Ice Data Center.
- Nathan, R., Getz, W.M., Revilla, E., Holyoak, M., Kadmon, R., Saltz, D., Smouse, P.E., 2008. A movement ecology paradigm for unifying organismal movement research. Proceedings of the National Academy of Sciences 105 (49), 19052–19059.
- Radford, A., Metz, L., Chintala, S., 2016. Unsupervised Representation Learning with Deep Convolutional Generative Adversarial Networks. <https://doi.org/10.48550/arXiv.1511.06434>.
- Roy, A., Fablet, R., Bertrand, S.L., 2022. Using generative adversarial networks (GAN) to simulate central-place foraging trajectories. Methods Ecol. Evol. 13, 1275–1287. <https://doi.org/10.1111/2041-210X.13853>.
- Santa Cruz, F., Ernst, B., Arata, J.A., Parada, C., 2018. Spatial and temporal dynamics of the Antarctic krill fishery in fishing hotspots in the Bransfield Strait and South Shetland Islands. Fish. Res. 208, 157–166. <https://doi.org/10.1016/j.fishres.2018.07.020>.
- Scott, D.W., 1979. On optimal and data-based histograms. Biometrika 66, 605–610. <https://doi.org/10.1093/biomet/66.3.605>.
- Tabetta, S., Suzuki, S., Nakamura, Y., 2015. Combined modeling of fish behavior and fishing operations for conger eel fishery in Ise Bay. Ecol. Model. 313, 266–275. <https://doi.org/10.1016/j.ecolmodel.2015.06.043>.
- Trathan P N , Fielding S, Hollyman P R, Murphy E J, Warwick-Evans V, Collins M A , Enhancing the ecosystem approach for the fishery for Antarctic krill within the complex, variable, and changing ecosystem at South Georgia, ICES Journal of Marine Science, Volume 78, Issue 6, September 2021, Pages 2065–2081, <https://doi.org/10.1093/icesjms/fsab092>.
- Wang, R., Zhu, G.P., 2019. Inferring behavior of Chinese krill fishing vessel using a simple walk model. J. Ocean Univ. China 18, 939–946. <https://doi.org/10.1007/s11802-019-3976-5>.
- Wadsworth, V., Constable, A., Dalla Rosa, L., Secchi, E.R., Seyboth, E., Trathan, P.N., 2022a. Using a risk assessment framework to spatially and temporally spread the fishery catch limit for Antarctic krill in the west Antarctic Peninsula: a template for krill fisheries elsewhere. Front. Mar. Sci. 9.
- Warwick-Evans, V., Fielding, S., Reiss, C.S., Watters, G.M., Trathan, P.N., 2022b. Estimating the average distribution of Antarctic krill *Euphausia superba* at the northern Antarctic Peninsula during austral summer and winter. Polar Biol. 45, 857–871. <https://doi.org/10.1007/s00300-022-03039-y>.
- Weninger, Q., Perruso, L., 2013. Fishing behavior across space, time and depth: With application to the Gulf of Mexico reef fish fishery. Work. Pap. - Dep. Econ. Iowa State Univ.
- Zhan, Y., Hu, D., Wang, Y., Yu, X., 2018. Semisupervised Hyperspectral Image Classification Based on Generative Adversarial Networks. IEEE Geosci. Remote Sens. Lett. 15, 212–216. <https://doi.org/10.1109/LGRS.2017.2780890>.